

Constraining the extension of a possible gamma-ray halo of 3C 279 from 2008–2014 solar occultations

Egor Kotelnikov¹, Grigory Rubtsov² and Sergey Troitsky^{2*}

¹*Physics Department, M.V. Lomonosov Moscow State University, Vorobjevy Gory, 119991, Moscow, Russia*

²*Institute for Nuclear Research of the Russian Academy of Sciences, 60th October Anniversary prospect 7a, 117312, Moscow, Russia*

2015 March 12, in original form 2014 December 03

ABSTRACT

The angular extension of the gamma-ray image of 3C 279 may be constrained by studying its solar occultations as suggested by Fairbairn et al. (2010). We perform this kind of analysis for seven occultations observed by Fermi-LAT in 2008–2014, using the Fermi-LAT Solar System tools. The results are interpreted in terms of models with extended gamma-ray halo of 3C 279; first constraints on the size and the flux of the halo are reported.

Key words: gamma-rays: general — magnetic fields — quasars: individual: 3C 279

1 INTRODUCTION

Some time ago, it was pointed out (Fairbairn et al. 2007) that one of the brightest gamma-ray sources in the sky, blazar 3C 279, is screened by the Sun every year. Since the Sun is not a very bright source of photons with energies $\gtrsim 100$ MeV, these events look as occultations and may be used to constrain some new models of physics and astrophysics. In particular, an extended halo of the source, if exists, would shine beyond the solar disk while the central point source is screened. Measurements of the gamma-ray flux of 3C 279 during the occultation may constrain (Fairbairn et al. 2010) the size and the flux of the extended halo in a way similar to the early measurements of angular diameters of stars in their lunar occultations, with the precision exceeding the angular resolution of the instrument.

Recently, the Fermi LAT collaboration has performed (Barbiellini et al. 2014) an analysis of four (2008–2011) solar occultations of 3C 279 and constrained the source flux during the periods when its center was screened. Barbiellini et al. (2014) have considered and constrained two scenarios: (i) transparency of the Sun for gamma rays and (ii) an extended sharp-edged disk with constant surface brightness and a priori fixed energy-dependent radius of $1.5^\circ \times (E/500 \text{ MeV})^{-1}$, where E is the gamma-ray energy. Nevertheless, there is a gap between these interesting results and constraints on realistic models of physics and astrophysics. We note that the solar transparency, case (i), as suggested by Fairbairn et al. (2007), requires an axion-like particle with parameters firmly excluded, since then, by several laboratory experiments, see e.g. Zavattini et al. (2008), Pugnat et al. (2008) and Ehret et al. (2010). The

extended halo, case (ii), if it exists, should be formed as a result of a random scattering process and is unlikely to look like a sharp-edged constant-intensity disk. The size of the halo is determined by a number of physical parameters of the source and/or of the intergalactic space, notably by the values of the magnetic fields. The halo extension is therefore an important observable to be constrained while it was kept a priori fixed in the analysis of Barbiellini et al. (2014).

In the present work, we fill this gap and follow the prescription of Fairbairn et al. (2010) more precisely; namely, we consider the halo size as a free parameter, while the halo shape is taken to be Gaussian. This approach opens a way to study and to constrain various models of the halo formation, as well as physical parameters of the source and the strength of the intergalactic magnetic field; note that the latter is a subject of intense debates. We make use of publicly available Fermi-LAT data for seven occultations (2008–2014) thus almost doubling the statistics as compared to four occultations used by Barbiellini et al. (2014).

2 DATA, ANALYSIS AND RESULTS

In this work, we use the Pass 7REP (V15) data of Fermi LAT (Atwood et al. 2009). We consider seven solar occultations of 3C 279 which happened on the 8th of October, 2008–2014. The precise periods of the occultations have been calculated with the help of the HORIZONS system (Giorgini et al. 1996). We processed the data with the standard *gtlike* routine from *Fermi Science Tools v9r32p5*¹. We use the “SOURCE” class photons with energies greater than 100 MeV. We apply standard quality cuts and require that

* E-mail: st@ms2.inr.ac.ru

¹ <http://fermi.gsfc.nasa.gov/ssc/data/access/>.

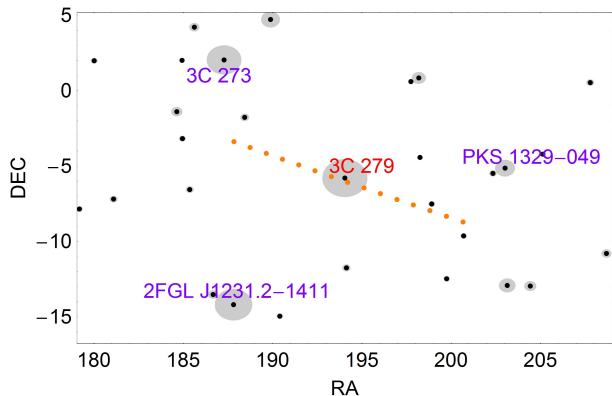


Figure 1. A map of the gamma-ray sky around 3C 279. Black dots correspond to gamma-ray sources listed in the 2FGL catalog (Nolan et al. 2012), the area of grey circles around them is proportional to their 2FGL flux. The solar path within ± 1 weeks from the occultation is shown by orange dots.

photon zenith angles with respect to the Earth do not exceed 100° and the satellite rocking angle is smaller than 52° .

Since we are interested in solar occultations, we need to disentangle fluxes of the Sun and of the blazar during the events. The Sun is a gamma-ray source firmly detected by Fermi LAT (Abdo et al. 2011), with the flux from the solar disk being produced by cosmic-ray interactions with the solar surface (Morris 1984; Hudson 1989; Seckel, Stanev & Gaisser 1991). Another, much more extended, flux component is caused by the inverse Compton scattering of cosmic-ray electrons on the solar light (Moskalenko, Porter & Digel 2006; Orlando & Strong 2007, 2008). At the time scales of order a week to a month, the flux of the quiet Sun is stable and may be determined by means of dedicated tools developed by the Fermi group for observations of moving targets, the Fermi-LAT Solar System Tools (Johannesson et al. 2013).

However, the time scale of an occultation, ~ 8.5 hours, is too short to determine its flux with the required accuracy. We, therefore, choose to study a four-week period surrounding each occultation, to determine the solar flux by means of the Solar System Tools. The tools assume that the solar flux is proportional to an average Fermi LAT solar flux. The spatial-spectral template of the moving Sun for the given time interval is produced with the *gtsuntemp* tool. The template allows to consider the Sun as an extended source in the *gtlike* tool, with the normalization treated as a free parameter. The template includes the solar disk as well as the extended emission with their energy and direction dependencies, while a single parameter, the overall flux normalization, is fitted. A complete model of the sky region includes Sun, galactic and isotropic diffuse components, 3C 279 and other point sources in the area of interest from the 2FGL catalog (Nolan et al. 2012). The solar path in the gamma-ray sky is sketched in Figure 1. The results are given in Table 1, together with 3C 279 fluxes for the same periods, quoted for reference². Then, we use this fixed solar flux in

² One may note that the solar flux quoted for 2013 was considerably higher than in other periods. We have traced the reason for this. Large solar flares, of M class and higher, are confirmed sources of energetic gamma rays, see e.g. Ackermann

Year	Flux, ± 2 weeks, $10^{-7} \text{ cm}^{-2} \text{ s}^{-1}$		Flux at occultation, $10^{-7} \text{ cm}^{-2} \text{ s}^{-1}$,
	Solar disk	3C 279	3C 279
2008	4.6 ± 0.4	3.6 ± 0.4	2.5 ± 2.6
2009	5.2 ± 0.5	7.1 ± 0.6	5.0 ± 5.3
2010	3.0 ± 0.4	8.1 ± 0.6	1.7 ± 4.6
2011	3.2 ± 0.4	2.6 ± 0.3	0.8 ± 1.5
2012	4.9 ± 0.4	2.4 ± 0.4	2.1 ± 2.7
2013	7.4 ± 0.4	6.2 ± 0.6	2.0 ± 2.1
2014	3.9 ± 0.4	3.8 ± 0.4	5.5 ± 3.1
stacked	4.7 ± 0.2	4.0 ± 0.2	2.6 ± 1.1

Table 1. Fluxes ($E > 100$ MeV) of the solar disk and of 3C 279, as determined for ± 2 weeks around the occultation, and of 3C 279 during the occultation; see the text for details of the account of the solar background. The flux of the solar extended emission, integrated over a large area up to 20° from the Sun, is 1.48 times the disk flux. The last row gives the fluxes for the sum of 7 stacked exposures.

the background model for the short-time observations during the periods when the point source at the position of 3C 279 was screened by the Sun. The flux of 3C 279 during the occultations, obtained in this way, is given in the last column of Table 1. Within the statistical errors, this flux is consistent with zero for each individual occultation, as one would expect for a usual point-like source. In order to achieve better precision, we merge the seven occultations with the following procedure:

- (i) the 7 photon files corresponding to the particular occultations are used jointly,
- (ii) the exposure cubes are coadded with the *gtlsum* tool,
- (iii) the 7 extended sources are included in the model, each representing the solar flux and the motion template for a particular year.

A stacked sum of all seven exposures results in a marginal excess of $(2.6 \pm 1.1) \times 10^{-7} \text{ cm}^{-2} \text{ s}^{-1}$, the 95% confidence level (CL) limit on the observed flux of 3C 279 when it is screened by the solar disk is thus rather weak,

$$F_{\text{obs}} < 4.8 \times 10^{-7} \text{ cm}^{-2} \text{ s}^{-1} \quad (95\% \text{ CL}). \quad (1)$$

The best-fit excess in the stacked occultation result, according to the *gtlike* tool, corresponds to ≈ 22 photons from the source while the number of background photons from the Sun is ≈ 90 . The stacked solar flux (both for the disk and for the extended emission), obtained in our fits, is (1.02 ± 0.04) times the value of Abdo et al. (2011).

To interpret the flux constraints in terms of the extended image, we simulate photons from a Gaussian ex-

et al. (2014). The enhancement of the solar flux in the 2013 period corresponds to a series of solar flares between the 9th and the 14th of October, 2013, recorded in the NOAA archive, <http://www.solarmonitor.org>. Both the detected flares and other unaccounted solar activity may affect systematically the signal and background estimates. We have checked that no flares were detected during all seven occultations and the systematic effect of the 2013 solar flares is within 10% in terms of the final result. We leave the investigation of a more detailed time-dependent solar flux model for future.

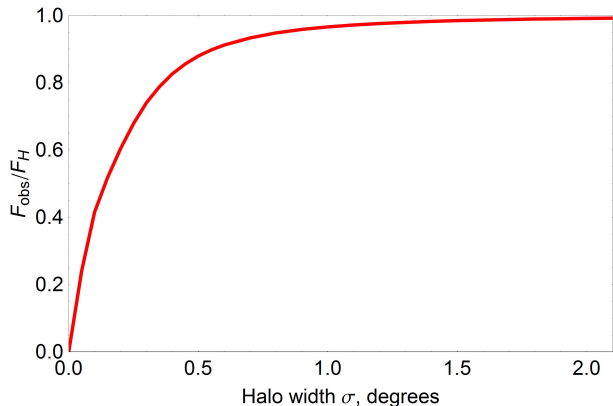


Figure 2. Fraction $F_{\text{obs}}/F_{\text{H}}$ of the flux of a Gaussian extended source centered at 3C 279 and not screened by the solar disk during the occultation, as a function of the image extension σ .

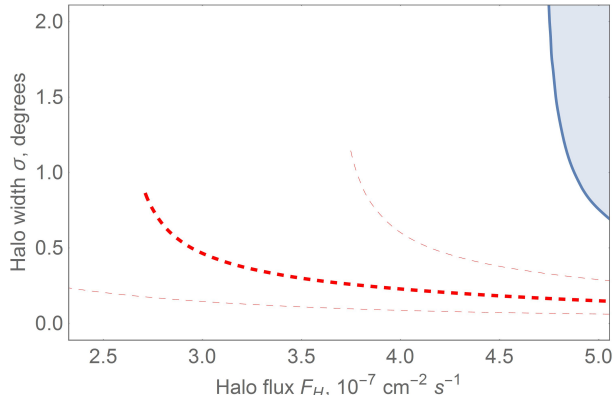


Figure 3. Constraints on the extension of the Gaussian halo of $E > 100$ MeV photons around 3C 279, as obtained in this work. Shaded area is excluded at the 95% confidence level; thick dashed line corresponds to the best-fit halo extension; thin dashed lines limit the 68% confidence-level range around the best fit.

tended source with the total flux F_{H} , centered at the position of 3C 279, with the extension σ . The flux density at the angular distance θ from the blazar is thus proportional to

$$\exp\left(-\frac{\theta^2}{2\sigma^2}\right).$$

Then we take into account the apparent motion of the Sun across the source and calculate the fraction of the simulated photons which are not screened by the solar disk during the occultation, when the central point is behind the Sun. This fraction, $F_{\text{obs}}/F_{\text{H}}$, is plotted in Fig. 2 as a function of σ . By making use of this plot, we directly constrain F_{H} and σ from F_{obs} , as prescribed by Fairbairn et al. (2010). The results are shown in Fig. 3, and these constraints on the extended image represent the main result of our present study.

3 CONCLUSIONS

In this Letter, we report on the analysis of Fermi-LAT data for seven solar occultations of 3C 279. Our results, expressed

in terms of the flux coming from the screened source, Table 1, are in agreement with earlier studies (four occultations seen by Fermi LAT, Barbiellini et al. (2014), and one occultation seen by EGRET, Fairbairn et al. (2007), reanalyzed with the account of the solar flux by Barbiellini et al. (2014)). However, we use these results, for the first time, to obtain constraints on the size of a possible extended gamma-ray halo of the source. These constraints are presented in the flux–extension parameter space, Fig. 3. Implications of these results for numerous particular models of the halo formation, see e.g. Aharonian, Coppi & Volk (1994), Gabici & Aharonian (2007), Atoyan & Dermer (2008), Neronov & Semikoz (2009) and numerous more recent elaborations, will be discussed elsewhere. It is interesting to note that, with the enhanced statistics we use (seven events versus four or one), a marginal excess consistent with the extended image is seen, though with a low statistical significance of ~ 2.4 standard deviations. This excess, if it were real, would be consistent with a halo of $\sim (0.5^\circ - 1^\circ)$ extension and $\sim (2 - 3) \times 10^{-7} \text{ cm}^{-2} \text{ s}^{-1}$ total flux, as well as with the solar transparency in the axion scenario (which predicts 1/3 of the photon beam to shine through the Sun³ but for which a consistent description in terms of a particle not excluded by laboratory experiments is missing). At higher energies, $E > 1$ GeV, the present statistics is too low to put an interesting limit. Further studies of solar occultations of 3C 279, notably in the pointing mode of Fermi LAT, and of the image extension of the blazar in its low state are needed in order to confirm or falsify these results.

ACKNOWLEDGMENTS

The authors are indebted to O. Kalashev for interesting discussions. This work was supported by the Russian Foundation for Basic Research, grant 13-02-01293 (adaptation of the method of solar occultations to the Fermi-LAT data, E.K.), and by the Russian Science Foundation, grant 14-12-01340 (constraining the extension of the gamma-ray image of the blazar 3C 279, G.R. and S.T.). G.R. acknowledges the fellowship of the Dynasty foundation. The analysis is based on data and software provided by the Fermi Science Support Center. The numerical part of the work has been performed at the cluster of the Theoretical Division of INR RAS.

REFERENCES

- Ackermann M. et al., 2014, ApJ, 787, 15
- Abdo A.A. et al., 2011, ApJ, 734, 116
- Aharonian F.A., Coppi P.S., Volk H.J., 1994, ApJ, 423, L5
- Atoyan A., Dermer C.D., 2008, ApJ, 687, L75
- Atwood W.B. et al., 2009, ApJ, 697, 1071
- Barbiellini G. et al., 2014, ApJ, 784, 118
- Ehret K. et al., 2010, PLB, 689, 149

³ Interestingly, the inverse-Compton emission is essentially zero in the direction of the solar disk, thus reducing the background in the searches for this effect (Orlando & Strong 2013). Just outside the disk, the emission from beyond the Sun returns to a significant level, so it is necessary to account for this background in the present study.

- Fairbairn M., Rashba T., Troitsky S., 2007, PRL, 98, 201801
- Fairbairn M., Rashba T., Troitsky S., 2010, MNRAS, 403, L6
- Gabici S., Aharonian F.A., 2007, ApSS, 309, 465
- Giorgini J.D. et al., 1996, BAAS 28(3), 1158; see <http://ssd.jpl.nasa.gov/?horizons>.
- Hudson, H.S., 1989, in *Gamma Ray Observatory Science Workshop Proceedings*, 4-351, NASA/GSFC.
- Johannesson G. et al., 2013, arXiv:1307.0197 .
- Morris D.J., 1984, JGR, 89, 10685.
- Moskalenko I.V., Porter T.A., Digel S.W., 2006, ApJ, 652, L65 (Erratum - 2007, ApJ, 664, L143).
- Neronov A., Semikoz D.V., 2009, PRD, 80, 123012
- Nolan P.L. et al. [Fermi LAT Collaboration], 2012, ApJS, 199, 31
- Orlando E., Strong A., 2007, ApSS, 309, 359
- Orlando E., Strong A., 2008, A&A, 480, 847
- Orlando E., Strong A., 2013, arXiv:1307.6798
- Pugnat P. et al. [OSQAR Collaboration], 2008, PRD, 78, 092003
- Seckel D., Stanev T., Gaisser T.K., 1991, ApJ, 382, 652
- Zavattini E. et al. [PVLAS Collaboration], 2008, PRD, 77, 032006

This paper has been typeset from a $\text{\TeX}/\text{\LaTeX}$ file prepared by the author.